

# Off axis tensile behaviour of cement matrix composites

E. De Bolster, K. Watzeels, H. Cuypers and J. Wastiels  
Department of mechanics and constructions, Vrije Universiteit Brussel, Belgium

**ABSTRACT:** The objective of this paper is to provide insight in a general characterization of the behaviour of unidirectionally glass fibre reinforced IPC (Inorganic Phosphate Cement) under off-axis tensile loading. This will be done through verification of currently existing theoretical models concerning fibre reinforced cementitious composites, explaining inconsistencies when they appear and giving a first general overview of damage mechanisms in order to make necessary interpretations. By testing the composite under tensile loading and measuring the strain with an extensometer, preliminary interpretation of the materials behaviour is made. A second series of specimens will be equipped with rosette strain gauges ( $0^\circ/90^\circ$ ) and subjected to tensile loading in order to capture the evolution of strain. Finally, an examination of the specimens will be performed, using a microscope and camera in order to come to better understanding of the evolution of the material during one loading sequence in case of off-axis loading. The study of simple unidirectionally reinforced specimens is used to obtain preliminary understanding of specimens with more complex reinforcement under multi axial loading.

## 1. INTRODUCTION

A renewed interest in the application of glass fibre reinforced concrete is recently slowly growing. The development of new protection layers for glass fibres and new low alkaline matrices provide better durability of these materials, which was the main reason why these materials have never been used in large-scale applications up to now. Like all other cementitious mixtures, Inorganic Phosphate Cement (IPC), a cementitious material developed at the “Vrije Universiteit Brussel”, Department of Mechanics of Materials and Constructions (MEMC), has high compressive strength but relatively low tensile strength. One of the major benefits of IPC compared to other currently existing cementitious mixtures is the non-alkaline environment of IPC before and after hardening. Ordinary E-glass fibres are thus not attacked by the matrix and can be used as reinforcement, with retention of the post-cracking stiffness and strength. The low viscosity of IPC allows typical fibre volume fractions of about 15% by hand lay-up, leading to tensile failure stresses above 100 MPa (when continuous aligned fibres are used).

The behaviour of unidirectional E-glass fibre reinforced IPC [1] is nearly linear elastic in uniaxial compression, while a significantly more complex non-linear behaviour is shown in uniaxial tension, due to multiple cracking of the matrix material (see figure 1). The non-linear stress-strain behaviour of IPC with aligned glass fibre reinforcement has already been analysed and modelled, in case loading is applied along the fibre axis [1].

The stress-strain behaviour under uniaxial loading can be divided in three zones ([2], [3]). The first zone characterizes the non-cracked specimens, when the bonding between the IPC-matrix and the glass fibres is assumed to be perfect and both work perfectly together to carry the entire load. The composite has a rather high stiffness  $E_{c1}$ . The second zone is the zone where multiple cracking occurs and the third zone is characterized as the post-cracking zone where the specimens are fully cracked and only the fibres that bridge those matrix micro cracks are responsible for the remaining strength and stiffness  $E_{c3}$ . Unlike the assumption made in [2] and [3], the multiple cracking doesn't occur at a certain stress, but the multiple cracking is rather a stochastic cracking over a certain range of strain ([1], [8], [9]).

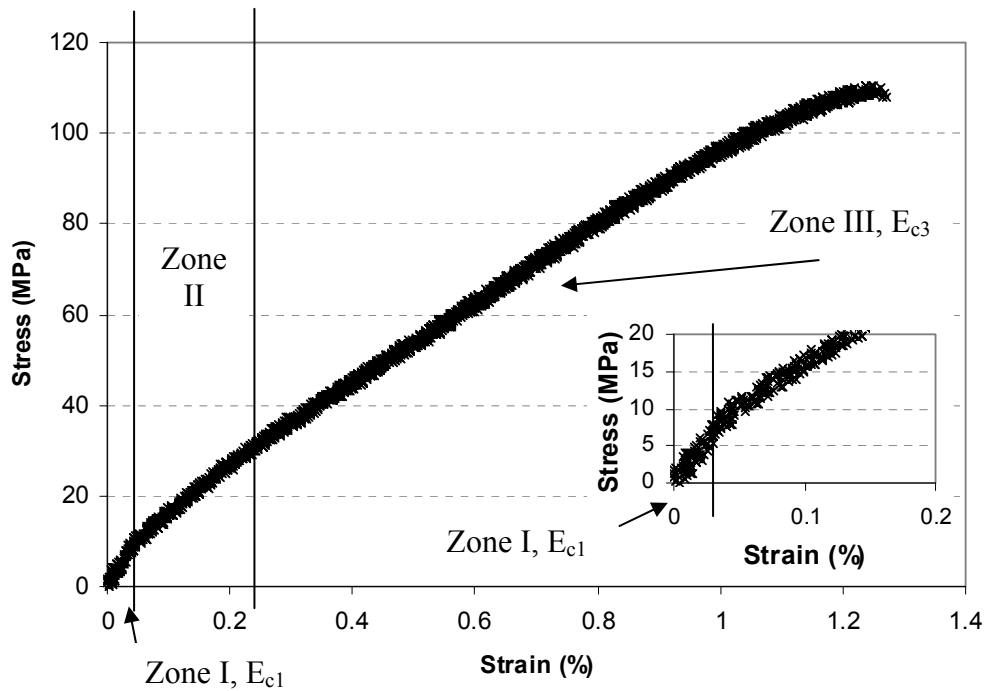


Figure 1: Typical stress-strain-curve of unidirectional E-glass fibre reinforced IPC.

In this paper, the behaviour of IPC with unidirectional reinforcement is studied under off-axis loading. This study has two aims:

- (i) study of the sensibility of cementitious materials with unidirectional reinforcement when the loading orientation differs slightly from pure alignment with the fibre axis, and
- (ii) gaining insight in the micro- and meso-mechanical phenomena occurring under complex loading with respect to the material axes in order to understand the introduction of damage in composites with bi-axial or random reinforcement under complex external load in a later step of the investigation.

## 2. EXPERIMENTAL PROGRAM

### 2.1. Methodology

Two series of glass fibre reinforced IPC specimens have been studied; both of them using continuous unidirectional reinforcement (UD). Different types of tests are performed on these series:

- (i) tensile test: The tests are performed with the tensile bench INSTRON 4505. This bench is used for static experiments and is able to apply a tensile loading of 100kN. The load cell used for these experiments can carry 10 kN. The speed, at which the test is performed, is 1 mm/min.
- (ii) microscopic examination: after subsequent loading steps (with increasing load) the surface of the specimens is examined through a microscope. At each of these loading steps a picture is taken, in order to get a visualization of the sequence of crack-manifestation.

The behaviour of unidirectional E-glass fibre reinforced IPC under off-axis tensile loading is characterized by verifying various behaviour models concerning fibre reinforced cementitious composites ([5],[6]). The experimental data is gathered on specimens with various off-axis

orientations ( $0^\circ$ ,  $7.5^\circ$ ,  $15^\circ$  and  $30^\circ$ ). The first series of specimens is used to gain macroscopic insight in the stress-strain behaviour. An extensometer (50 mm gage length) is applied along the loading axis of the specimens and measures the average strain from both sides of the specimen. The second series of specimens is used to gain more detailed insight in the stress-strain behaviour. Here, a rosette strain gauge ( $0^\circ$ ,  $90^\circ$ ) at each side of the specimen is used to measure the longitudinal and transversal strains. Yet again, it is the average of both measured strains that is used to study the behaviour. At the same time the second series of specimens is subjected to microscopic visualization of the surface of the specimens, in order to capture the cracking-sequence.

## 2.2. Specimens

The fabrication method used, is hand lay-up. Each laminate consists of 5 layers of glass fibre rovings. The unidirectional reinforcement has a fibre density of  $158\text{g/m}^2$ , of which  $141\text{g/m}^2$  is present as reinforcement in the main direction and  $17\text{g/m}^2$  of the reinforcement is aligned along the transverse direction. A matrix density of  $700\text{g/m}^2$  is used. All specimens have a length of 300 mm, in order to create a uniform stress distribution in the middle of the specimen.

At least nine specimens are cut from each laminate. Six of them are cut parallel to the fibre axis and used as reference-specimens. These give the material characteristics of the laminate. The others are cut, so as to obtain the desired off-axis-orientation. For laminates 1 and 4 this off-axis-orientation is  $30^\circ$ . For laminates 2 and 5 it is  $15^\circ$  and for laminates 3 and 6 an off-axis-orientation of  $7.5^\circ$  is realized. The total amount of off-axis specimens for laminates 1,2 and 3 is six (three small ones and three larger ones). For laminates 4, 5 and 6 there are only three specimens for off-axis testing.

Series 1	Orientation $\theta$ ( $^\circ$ )	Width (mm)	Thickness (mm)	Fibre volume fraction (%)	Series 2	Orientation $\theta$ ( $^\circ$ )	Width (mm)	Thickness (mm)	Fibre volume fraction (%)	
L1-UD	0	19.61	2.23	12.5	L4-UD	0	20.19	2.22	12.5	
L1-30	30	20.19	2.40	11.5	L4-30	30	20.41	2.39	11.6	
L1-30w	30	47.88	2.46	11.3						
<b>average</b>			<b>2.36</b>	<b>11.8</b>	<b>average</b>			<b>20.27</b>	<b>2.28</b>	<b>12.2</b>
L2-UD	0	19.99	2.15	12.9	L5-UD	0	20.09	2.14	12.9	
L2-15	15	20.15	2.37	11.7	L5-15	15	20.27	2.35	11.8	
L2-15w	15	47.85	2.42	11.5						
<b>average</b>			<b>2.31</b>	<b>12.0</b>	<b>average</b>			<b>20.15</b>	<b>2.21</b>	<b>12.6</b>
L3-UD	0	19.90	2.22	12.5	L6-UD	0	20.04	2.23	12.5	
L3-75	7.5	20.33	2.59	10.7	L6-75	7.5	20.38	2.46	11.3	
L3-75w	7.5	48.29	2.49	11.2						
<b>average</b>			<b>2.43</b>	<b>11.5</b>	<b>average</b>			<b>20.15</b>	<b>2.31</b>	<b>12.1</b>

Table 1. Average width, thickness and fibre volume fraction of UD-reinforced specimens, series 1 and 2.

Table 1 summarizes the average fibre volume fraction, thickness and width of the test specimens of each laminate. On average, a fibre volume fraction of 11.8% (series 1) and 12.3% (series 2) is obtained. Table 2 summarizes the material characteristics of the components of glass fibre reinforced IPC.

Component	Tensile strength (MPa)	E-modulus (GPa)	Density (kg/m <sup>3</sup> )
IPC	10	18	1600-1900
glassfibre	1400	72	2540

Table 2. Material characteristics of the components of glass fibre reinforced IPC.

## 2.3. Results

### 2.3.1. Series 1

The first series of specimens is used to gain insight in the overall macroscopic behaviour of glass fibre reinforced IPC under off-axis-loading. Tensile tests and the use of an extensometer (50 mm gage length) allow to create stress-strain-curves for each orientation (see figure 2). The extensometer is applied along the loading axis.

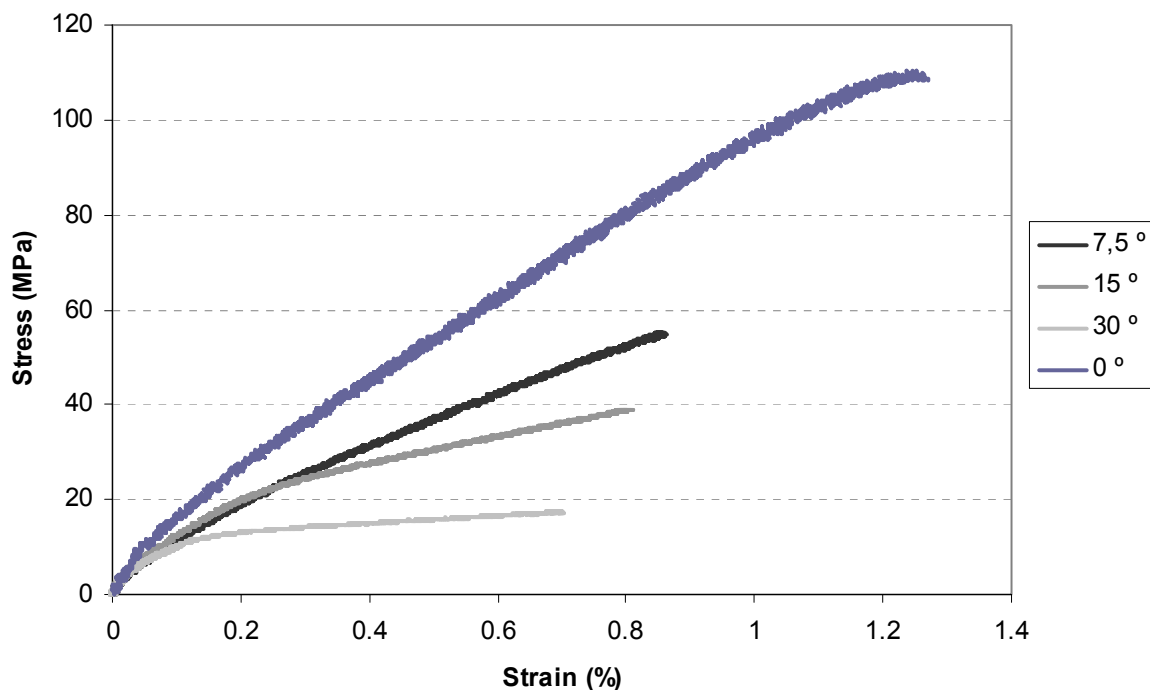


Figure 2: Typical stress-strain-curve of glass fibre reinforced IPC under off-axis-loading.

All curves show a similar tendency on their stress-strain-curve. Initially, the specimens show a rather high stiffness  $E_{c1}$ . When a loading of 5 MPa and higher is applied, this high stiffness reduces gradually until a constant lower stiffness value is reached. The reduction in stiffness is dependent on the off-axis-orientation: the higher this orientation, the lower the stiffness in the third zone  $E_{c3}$  (see table 3 and table 4).

Off-axis orientation (°) (series 1)	$E_{c1}$ (GPa)		$E_{c3}$ (GPa)	
	average	stdev	average	stdev
0	25.0	2.6	8.37	0.30
7.5	20.2	1.3	5.41	0.05
15	21.7	5.1	2.40	0.19
30	19.8	2.3	0.83	0.03

Table 3. Average stiffness of the off-axis-specimens (series 1, width 20 mm) in the first and third zone.

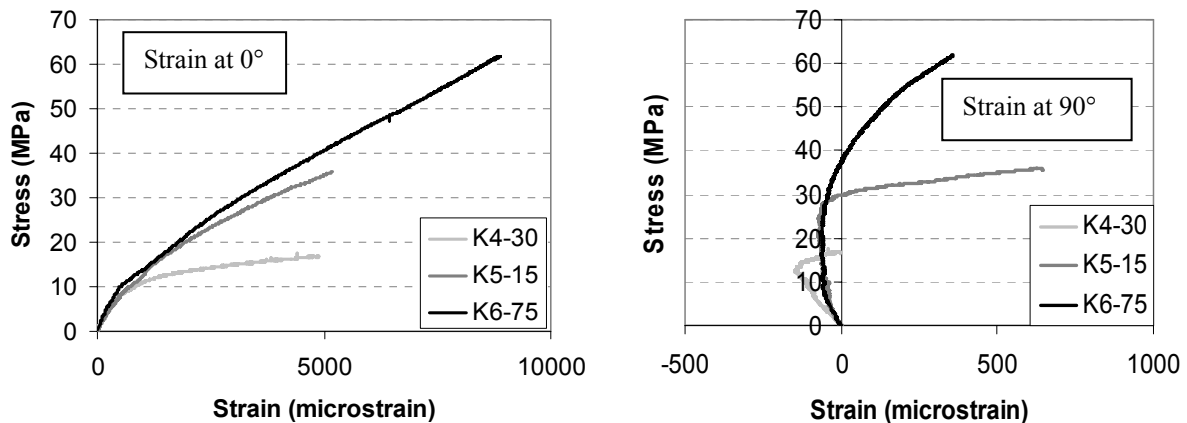
Off-axis orientation (°) (series 1)	$E_{c1}$ (GPa)		$E_{c3}$ (GPa)	
	average	stdev	average	stdev
7.5	19.8	1.5	5.50	0.50
15	19.8	1.2	2.50	0.50
30	19.0	0.9	1.18	0.03

Table 4. Average stiffness of the off-axis-specimens (series 1, width 48 mm) in the first and third zone.

Comparison between table 3 and table 4 shows that in general the specimens don't need to be wider than 20 mm in order to accurately determine the stiffness in the first and third zone. Only the specimens with a width of 48 mm, cut at 30° show discrepancy compared to specimens of 20 mm width, which is slightly higher than the standard deviation. Because of the good resemblance of specimens with different width, only specimens with 20 mm width will be used in the second series.

### 2.3.2. Series 2

The strains of the second series of specimens were measured with rosette (0, 90°) strain gauges to fully capture the deformation behaviour. They are also tested on the tensile bench. Moreover, at regular stress-intervals microscopic visualization of the surface of the specimens was established, in order to capture the cracking-sequence.



**Figure 3: Stress-strain-curves for varying off-axis-orientation**  
**Left: longitudinal stress versus longitudinal strain**  
**Right: longitudinal stress versus transversal strain**

The strain behaviour of unidirectional glass fibre reinforced IPC reflects the crack-introduction in the multiple cracking zone and in the post-cracking zone (see figure 3), no matter what the angle between the loading and fibres is. In the pre-cracking zone the material will behave as a linear elastic material: the strain at 0° is tensile, while the strain at 90° of course shows opposite tendency. As soon as cracks are introduced into the matrix material, the stress distribution changes: the stress in the fibres will increase and the stress in the matrix will decrease, leading to a relaxation of the compressive strain at 90° (see figure 3 on the right). The tensile strains at 90° at the end of the loading cycle are due to the release of internal stresses caused by shrinkage (see 2.4.2), which were present in the unloaded

specimens and are released once multiple cracking is introduced in the matrix (matrix stresses will then go to zero).

## 2.4. Analysis

### 2.4.1. Macroscopic behaviour

*Pre-cracking zone:  $E_{c1}$*

A theoretical prediction of the stiffness in the pre-cracking (linear elastic) zone has been proposed by [7], and is presented in the following equations:

$$E_{c1} = E_m V_m + \eta_l \eta_\theta E_f V_f \quad (1)$$

$$\eta_\theta = \sum a_\theta \cos^4 \theta \quad (2)$$

$$\eta_l = 1 \quad (3)$$

In these equations  $E_m$  and  $E_f$  represent the stiffness of the matrix and the fibres respectively;  $V_m$  and  $V_f$  are the matrix volume fraction and the fibre volume fraction;  $\eta_\theta$  and  $\eta_l$  are the efficiency factors that reflect the effect of the fibre orientation and the effect of the fibre length;  $\theta$  is the fibre orientation and  $a_\theta$  is the fraction of fibres that is aligned in the specified fibre orientation. Verification of the model with the experimentally obtained data gives fairly accurate results (figure 4).

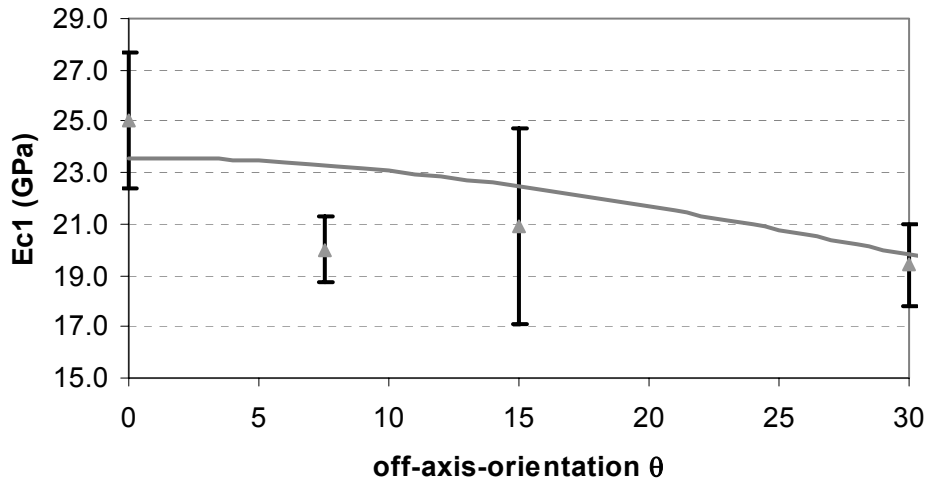


Figure 4: Initial stiffness off-axis-specimens: Experimental data versus theoretical prediction (1)  
Experiments: triangles + standard deviation; Theory: grey line

*Post-cracking zone:  $E_{c3}$*

In [5] a theoretical prediction of the tensile strength  $\sigma_{cu}$ , based on the assumption that it is local bending of the fibres in the vicinity of a matrix crack which is the main mechanism determining the behaviour of the composite, was developed. This phenomenon of local fibre bending (see figure 5) could also be an important factor that influences the post-cracking stiffness. Another possible explanation for the strongly post-cracking stiffness can be

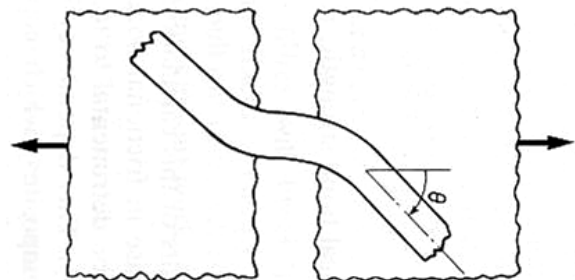


Figure 5: Realignment of the fibers in the loading direction, on a local level.

found: the glass fibre reinforcement of the specimens used consists of fibre bundles instead of single fibres. It might be possible that the reinforcement of a fibre bundle performs worse than a single fibre, when it comes to post-cracking stiffness.

*Post-cracking zone:  $\sigma_{cu}$*

Usually, for a composite (which is not isotropic), the Tsai-Hill-criterium is applied to get a prediction of the failure-stress of a composite. The equation of the curve composite strength versus off-axis-orientation can be derived [4] and gives:

$$\sigma_{cu} = \frac{1}{\sqrt{\left(\frac{\cos^2 \theta}{\sigma_{1Tu}}\right)^2 - \frac{\cos^2 \theta \sin^2 \theta}{\sigma_{1Tu}^2} + \left(\frac{\sin^2 \theta}{\sigma_{2Tu}}\right)^2 + \left(\frac{\cos \theta \sin \theta}{\tau_{12u}}\right)^2}} \quad (4)$$

In equation (4) three different strengths of the material play a role:  $\sigma_{1Tu}$  (longitudinal tensile strength),  $\sigma_{2Tu}$  (transversal tensile strength) and  $\tau_{12u}$  (shear strength). The compressive strengths don't have any influence because of the tensile nature of the test. These strengths are on one hand obtained through direct experimental measurements (for  $\sigma_{1Tu}$  and  $\sigma_{2Tu}$ ) and on the other hand through experimental curve-fitting: fitting of equation (4) with experimental data and considering  $\tau_{12u}$  as the unknown parameter.

The results obtained are:  $\sigma_{1Tu} = 106.5$  MPa,  $\sigma_{2Tu} = 10.3$  MPa and  $\tau_{12u} = 8$  MPa.

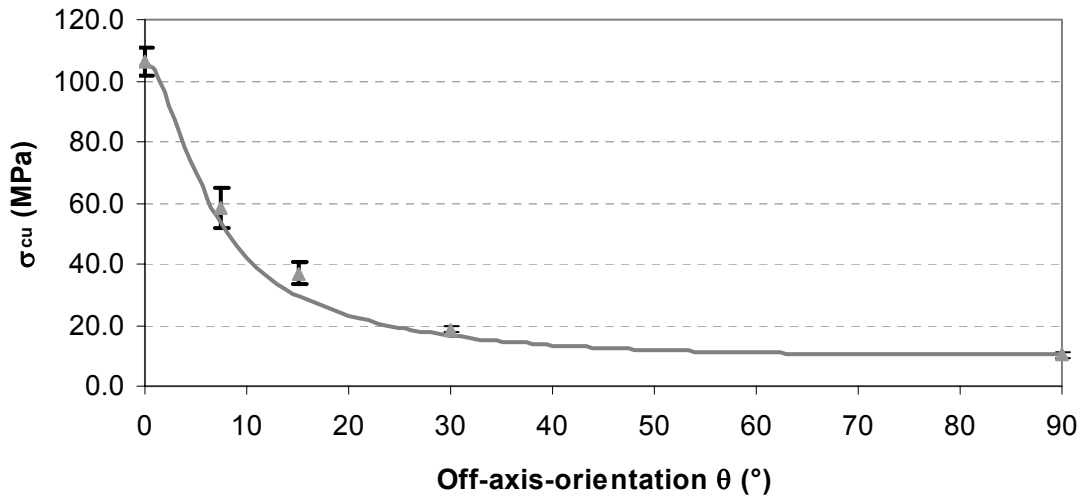


**Figure 6: Failure stress off-axis-specimens: Experimental data versus theoretical prediction (4)**  
Experiments: triangles + standard deviation; Theory: grey line

Verification of the model with the experimental obtained data gives fairly accurate results (figure 6). The curve indeed strives to an asymptotic level of tensile transversal stress.

For the interpretation of this curve, care must be taken:

- i) the shear strength has been obtained through an optimisation of a curve.
- ii) one of the hypotheses of the Tsai-Hill-criteria is that the bonding between matrix and fibres is perfect from the beginning of the loading until the specimen breaks. This hypothesis is only applicable in the first zone of the tensile stress-strain-behaviour of an IPC-composite. From the second zone on, the perfect bond has been replaced by friction. This friction does represent some kind of bonding, but it isn't a perfect one.

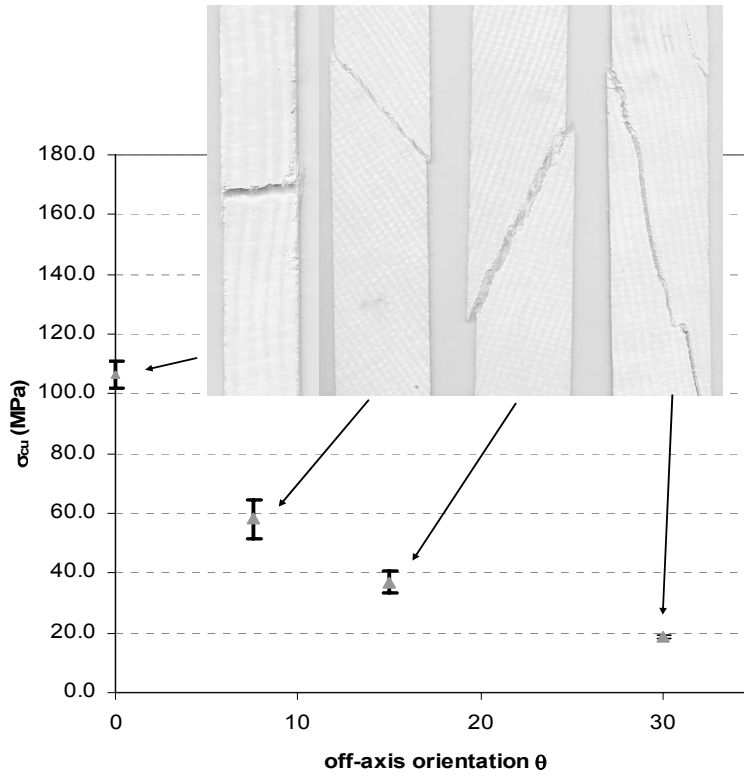


Figure 7: Failure mode of varying off-axis-orientation ( $0^\circ$ ,  $7.5^\circ$ ,  $15^\circ$  and  $30^\circ$ )

Because of the interactive nature between the stresses of the Tsai-Hill-criterion, it is impossible to derive a single failure mode for all tested specimens from a value obtained by equation (4). Figure 7 however, does give some indication about the main failure mode (term with highest influence in equation (4)). The reference-specimens (UD) will obviously fail because the longitudinal tensile strength is exceeded. The off-axis-specimens will mainly show shear failure.

#### 2.4.2. Microscopic behaviour

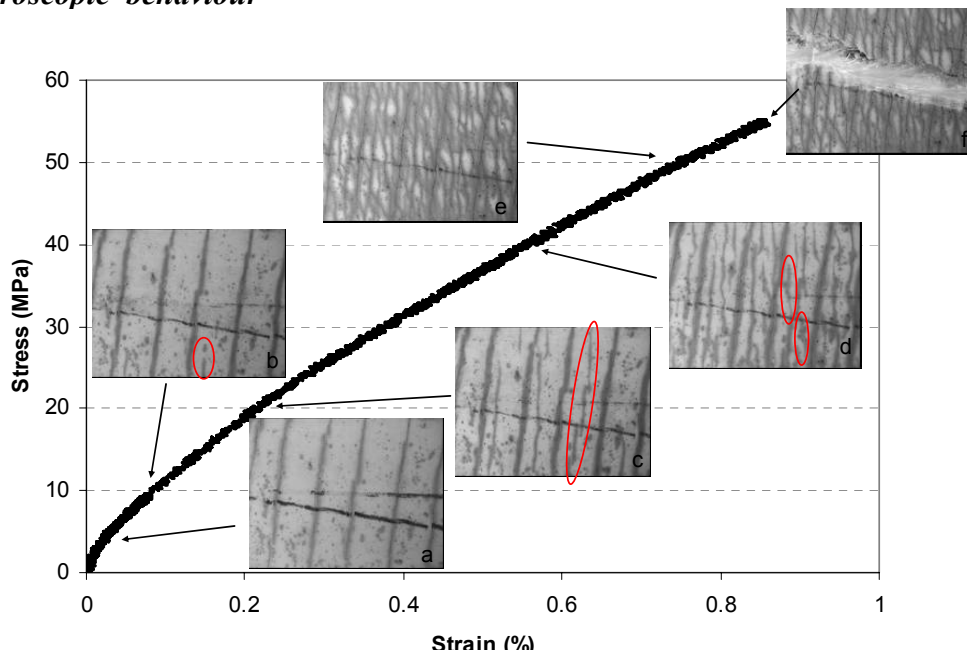


Figure 8. Crack-sequence

For each fibre orientation the same sequence of phenomena is observed, but the stress at which these phenomena occur varies with varying fibre orientation. Figure 8 shows the crack-sequence of one of the specimens with an off-axis orientation of  $7.5^\circ$ . The same tendency can be found for the other off-axis orientations. The horizontal black line represents the loading direction. The inclined black line represents the fibre-alignment of the specimen.

The sequence of damage consists of:

- (i) Shrinkage cracks (damage at 0 MPa), see figure 8a. This damage occurs perpendicular to the fibre alignment and is the result of loads imposed by the fabrication: restrained shrinkage of the IPC-matrix and internal stresses caused by cutting the specimens. For  $7.5^\circ$ -off-axis specimens the average crack distance is 2.94mm, with a standard deviation of 0.63.
- (ii) Primary cracks (damage at about 5 MPa), see figure 8b. They appear perpendicular to the loading direction. The cracks submerge in the middle of the matrix-blocks created by the shrinkage cracks. With increasing stress, new primary cracks occur and the existing ones grow until they reach a shrinkage crack (see figure 8c and figure 8d). An average crack distance of 1.00mm, with a standard deviation of 0.16 is measured on the  $7.5^\circ$ -off-axis specimens.
- (iii) Secondary cracks (damage at higher stresses), see figure 8e. These cracks propagate at the edges of the shrinkage cracks or the primary cracks. These cracks are probably introduced due to the effect of local bending of the fibre bundles at the crack face. The fibre bundles that bridge the primary cracks show a tendency to align in the loading direction. This induces new tensile stresses in the matrix and – consequently – new cracks.
- (iv) Failure. The unidirectional loaded specimen will fail due to fibre fracture perpendicular to the loading direction. The off-axis loaded specimens however show a rather different failure mode (see figure 7). The fracture occurs along the fibre. A part of the fibre bundle bridges the fracture, while the rest stays imbedded in the matrix. There is only a relatively small part of the fibres (at the edge of the specimen) that gets pulled out. The fibre itself is not subjected to any fracture (see figure 8f).

### 3. CONCLUSIONS

Unidirectional glass fibre reinforced IPC, which is subjected to off-axis loading, shows a similar non-linear behaviour as when subjected to loading along the fibre axis. Initially, the stress-strain-curve exhibits a linear elastic behaviour (zone I), which is followed by a transitional zone where multiple cracking occurs (zone II) and a second linear zone with reduced stiffness and strength (zone III). The post-cracking zone (zone III) abruptly ends, when failure occurs along the fibre orientation, but the fibre itself is not subjected to any fracture.

Fracture occurs after three different damage phenomena have appeared. First, there are shrinkage cracks. These cracks are due to internal stresses, caused by restrained shrinkage of the matrix. As the stress level increases, primary cracks appear and propagate perpendicular to the loading direction. At last, secondary cracks appear prior to final failure.

Theoretical prediction of the stiffness in the first zone gives fairly good accordance to the experimental data. The complex nature of the crack pattern (shrinkage cracks, primary cracks, secondary cracks, crumbling of the matrix, ...) is certainly an indication of the complex stress distribution that leads to the strongly decreased post-cracking stiffness in the third zone. A solid theoretical prediction that accounts for all of these influences is under development.

Theoretical prediction of the failure stress, however, again give fairly good accordance to the experimental data.

## ACKNOWLEDGMENT

Financial support from the Institute for the Promotion and Innovation by Science and Technology in Flanders (“IWT-Vlaanderen”) is gratefully acknowledged.

## REFERENCES

- [1] Cuypers, H., “Analysis and Design of Sandwich Panels with Brittle Matrix Composite Faces for Building Applications”, Phd thesis, Vrije Universiteit Brussel, Belgium (2002)
- [2] J. Aveston, G.A. Cooper and A. Kelly, “*Single and multiple fracture*”, The properties of Fibre Composites, Proc. Conf. National Physical Laboratories, IPC Science & Technology Press Ltd. London (1971)
- [3] J. Aveston and A. Kelly, “*Theory of multiple fracture of fibrous composites*”, J. Mat. Sci., Vol. 8 (1973)
- [4] Matthews, F.L. and Rawlings, R.D., “Composite Materials: engineering and Science”, Chapman and Hall (1994)
- [5] Aveston, J., Mercer, A.R. and Sillwood, J.M., “Fibre Reinforced Cements – Scientific Foundations for Specification”, Composites – Standard, Testing and Design, Proc. National Physical Laboratory Conference, Sci and Technology Press (1974)
- [6] Bentur, A. and Mindess, S., “Fibre Reinforced Cementitious Composites”, Elsevier Applied Science (1990)
- [7] Krenchel H., “Fibre Reinforcement”, Akademisk Forlag, Copenhagen (1964)
- [8] Cuypers H. and Wastiels J., “Application of a stochastic matrix cracking theory on E-glass fibre reinforced cementitious composites”, *Proceedings of 10th European Conference on Composite Materials (ECCM10), Brugge, Belgium, june 3-7 2002, paper 305, 10 pp (CD-ROM).*
- [9] Cuypers H., Van Hemelrijck D., Dooms, B., Wastiels J., ”Determination of stochastic matrix cracking in brittle matrix composites”, *Proc. 3<sup>rd</sup> Int. Conf. on emerging technologies in NDT, Tessaloniki, 26-28 May 2003, pp.53-59*